

INFLUENCE OF BOUNDARY CONDITIONS ON THE LARGE-SCALE STRUCTURES IN TURBULENT PLANE COUETTE FLOW

M. Lygren and H.I. Andersson

Division of Applied Mechanics
Norwegian University of Science and Technology
N-7491 Trondheim, NORWAY

ABSTRACT

Two new sets of boundary conditions have been devised with the view to break the inflow-outflow coupling associated with periodic boundary conditions. This coupling is believed to play a significant role in the formation of large-scale structures found in numerically generated turbulent plane Couette flow. Direct numerical simulations are here performed in order to investigate the influence of the new boundary conditions on these large-scale structures. The effect of the boundary conditions was to shorten the streamwise lengthscale of the structures as well as reducing the inclination for roll cells to develop.

BACKGROUND AND MOTIVATION

Recent experimental studies have shown the existence of elongated structures involved in the destabilization process of a slightly modified laminar plane Couette flow; cf. Dauchot and Daviaud (1995) and Bottin et al. (1998). These structures were in the form of streaks originating from pairs of counter-rotating streamwise vortices. The modification of the pure Couette flow was accomplished by introducing a thin spanwise wire in the central plane. Bottin et al. (1998) conjectured that the vortices exist as nonlinear solutions in the limit of wire diameter going to zero.

Linear stability analysis of the plane Couette flow indicates that this flow is stable with respect to infinitesimal perturbations at all Reynolds numbers, thus making this flow a prototype of flows experiencing subcritical transition to turbulence. Cherhabili and Ehrenstein (1997) searched for finite-amplitude solutions that could destabilize the laminar flow. By adding a streamwise pressure gradient to the flow they found in the pure

Couette limit structures that were periodic in the spanwise direction and spatially localized in the streamwise direction. These structures were in the form of counter-rotating vortices.

Direct numerical simulations (DNS) have shown that very large elongated flow structures, as compared with other wall-bounded turbulent flows, are present in numerically simulated plane turbulent Couette flows. Miyake et al. (1987), Lee and Kim (1991), Bech and Andersson (1994) and Papavassiliou and Hanratty (1997) moreover observed a persistent pattern of counter-rotating streamwise-oriented vortices or roll cells. Similar vortex patterns were also observed by Kristoffersen et al. (1993), Bech et al. (1995) and Komminaho et al. (1996), but the roughly circular vortices were neither persistent in time nor in space. This latter observation is also consistent with recent flow visualizations and correlation measurements by Bech et al. (1995) and Tillmark and Alfredsson (1998).

Bech and Andersson (1994) and Komminaho et al. (1996) also examined the effect of the finite computational domain inevitably used in DNS. By using different computational boxes up to 5 (Bech and Andersson, 1994) and 42 (Komminaho et al., 1996) times the size of that used in the channel flow simulation by Kim et al. (1987), it was found that the box size had a significant influence on the large-scale structures in turbulent Couette flow. More recently, it was conjectured by Andersson et al. (1998) that the persistent roll cells observed independently in some of the DNSs are a numerical artifact rather than a physical reality and the following hypothesis was put forward:

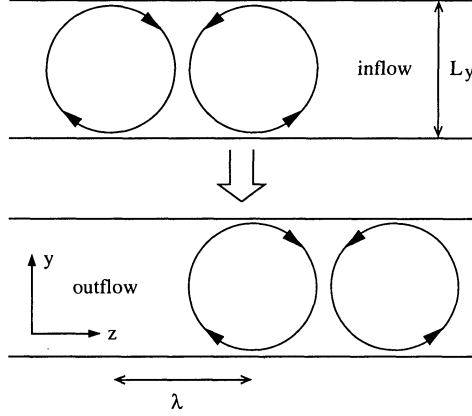


Figure 1: Effect of translational boundary conditions on a pair of counter-rotating vortices.

The counter-rotating streamwise vortices observed in numerically generated turbulent plane Couette flow is a spurious flow phenomenon. The origin of these roll cells is the localized elongated vortical structures found in the perturbed laminar Couette flow, which are believed to be present also in the turbulent flow regime. The use of periodic boundary conditions in the streamwise direction provides a mechanism for self-amplification of these large-scale vortices, which eventually develop into a roll-cell pattern which extends throughout the entire computational domain.

The objective of the present study is to further investigate the role of inflow - outflow boundary conditions on the large-scale structures and, in particular, on the possible generation of counter-rotating roll cells. With the view to break the inflow-outflow coupling the conventional periodic (i.e. cyclic) boundary conditions, which have become the prevailing practice in DNS, are replaced by a set of non-repetitive boundary conditions.

NUMERICAL APPROACH AND NON-PERIODIC BOUNDARY CONDITIONS

The direct simulations were accomplished with the finite-difference code MECCLES (Modified Explicit Channel Code originally developed for Large Eddy Simulation) (Andersson et al., 1998) with second-order accurate central-difference approximations in space and a second-order Adams-Bashforth scheme in time. The Poisson equation for the pressure field was solved by a multigrid scheme using repeated V-cycles and Line Zebra Gauss-Seidel iterations as the smoother. MECCLES is therefore more versatile than its parent code ECCLES (Gavrilakis et al., 1986), which uses FFTs in the two homogeneous coordinate directions.

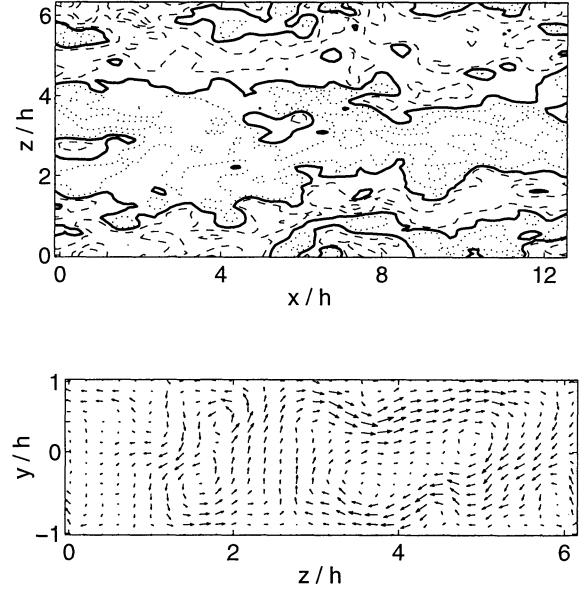


Figure 2: From DNSM. Top: Instantaneous streamwise velocity at the center plane. Bold lines separate regions of positive and negative fluctuations. Bottom: Secondary structures. Velocity field averaged in streamwise direction.

The time-dependent three-dimensional Navier-Stokes equations for incompressible fluid motion were integrated numerically on a region between two parallel planes, one of which is moving with constant speed U_w and the other being stationary. The Reynolds number $Re = U_w h / 2\nu$ was 1300. Here h is half the distance between the plates and ν is the kinematic viscosity. The computational domain in the streamwise (x), wall-normal (y) and spanwise (z) directions was $4\pi h \times 2h \times 2\pi h$, making the aspect ratio L_z/L_y equal to π . The number of grid points $I \times J \times K$ was $96 \times 64 \times 64$. No-slip conditions were imposed on the velocity components at the solid walls and the conventional periodicity was retained in the spanwise direction. As replacement for the periodic boundary conditions in the streamwise direction, two different sets of non-repetitive inflow-outflow conditions were used. First, the outflow boundary conditions were taken as the mirror image of the primitive variables about the vertical midplane of the inlet flow field (M):

$$\left. \begin{aligned} f_{1,j,k} &= f_{I-1,j,K-k+1} \quad (\text{inflow}) \\ f_{I,j,K-k+1} &= f_{2,j,k} \quad (\text{outflow}) \end{aligned} \right\} f = u, v, p,$$

$$\left. \begin{aligned} f_{1,j,k} &= -f_{I-1,j,K-k+2} \quad (\text{inflow}) \\ f_{I,j,K-k+2} &= -f_{2,j,k} \quad (\text{outflow}) \end{aligned} \right\} f = w.$$

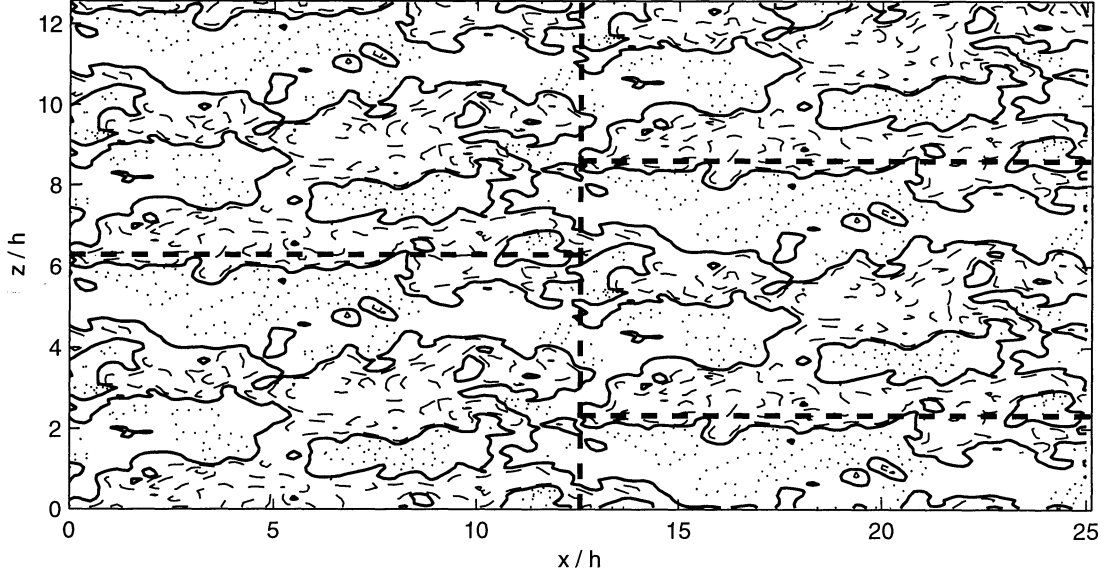


Figure 3: Instantaneous streamwise velocity field in the center plane, DNST. The area on the image is four times (i.e. $2L_x \times 2L_z$) the area of the computational domain. Duplication is done in accordance with the boundary conditions. Bold dashed lines indicate the boundary of the computational area.

Alternatively, the instantaneous inflow was translated a distance $\lambda = N_\lambda \cdot \Delta z$ in the spanwise direction to become a proper outflow field (T):

$$\left. \begin{aligned} f_{1,j,k} &= f_{1-1,j,k+N_\lambda} \quad (\text{inflow}) \\ f_{1,j,k+N_\lambda} &= f_{2,j,k} \quad (\text{outflow}) \end{aligned} \right\} f = u, v, w, p.$$

The amount of spanwise translation λ is an essential control parameter. $\lambda \approx L_y$ would be an optimum choice in order to break the artificial amplification mechanism which has been responsible for the generation of a persistent roll-cell pattern in some earlier DNSs of plane Couette flow. This can be seen in Figure 1 where a pair of counter-rotating cells in the inflow plane is translated a length $\lambda = L_y$ in the outflow plane. This translation will clearly suppress the generation of elongated vortices in the streamwise direction. However, the multigrid Poisson solver restricts the number of points N_λ associated with the spanwise translation λ . Multigrid techniques are most efficient when we can zoom down to a coarse grid. Ideally N_λ (and I, J, K) should be a multiple of 2. N_λ was chosen to be 24 thus giving an efficient multigrid solver and $\lambda = N_\lambda L_z / K = 1.18 L_y$. It is particularly noteworthy that the translational-type boundary conditions with $N_\lambda = 24$ introduce a streamwise periodicity $8L_x$ since the fraction $N_\lambda / K = 24/64$ needs to be multiplied by

8 to give an integer number.

RESULTS AND DISCUSSION

Simulations have been performed with each of the two new boundary conditions. The number of grid points and the size of the computational domain described in the previous section were the same as in the DNS with ordinary periodic boundary conditions reported by Kristoffersen et al. (1993). For convenience, we denoted this simulation DNSP. The simulation with M(T)-type boundary conditions is called DNSM(DNST). The initial data of the simulations were random fluctuations superimposed on a linear profile. After the simulations reached a statistically steady state, statistical data were recorded during the following 1000 dimensionless time units. Here and in the following the time scale is normalized with the friction velocity $u_\tau = \sqrt{\tau_w / \rho}$ and the kinematic viscosity.

The simulation with the M-type boundary conditions showed that these boundary conditions did not prevent elongated structures to fill the whole length of the computational domain. An instantaneous view of the streamwise fluctuating velocity in the center plane in Figure 2 shows these large structures in the form of wide bands of high and low speed fluid. These struc-

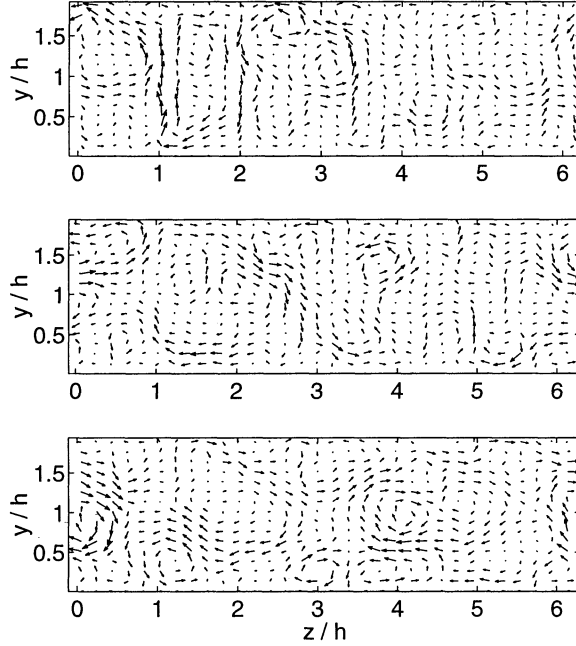


Figure 4: Time history of x-averaged secondary structures, DNST. From top to bottom the images are taken at $T=1374, T=1414, T=1455$.

tures evolved very slowly and were formed near the end of the simulation. After they were established they kept their spanwise location in the xz -plane. The M-type boundary conditions allow structures to fill the length of the computational domain if they have reflection symmetry about the vertical xy -midplane. After the structures in Figure 2 showed up, they were therefore “locked” in their position by the boundary conditions.

The accompanying vortical flow pattern in the cross-sectional plane, as shown in Figure 2, was neither persistent in time nor space, i.e. in accordance with the DNSs reported by Bech et al. (1995); Kommihio et al. (1996); Kristoffersen et al. (1993). Although there was localized secondary vortical motion, distinct pairs of counter-rotating cells could not be identified. The typical velocity associated with the vortical motion was about 1% of U_w .

In contrast to DNSP and DNSM, the translational boundary conditions prevented the streaks in the channel center from obtaining an infinite length. These streaks could reach through the computational domain, but the boundary conditions still gave them a finite length in streamwise direction. This is exemplified in Figure 3 where a snapshot of the streamwise velocity is duplicated in accordance with the boundary conditions.

The vortical flow pattern in the simulated flow using the translational boundary conditions differed from the pattern in DNSM in the sense that the vortices were smaller and less organized. Examples of this are given in Figure 4 where a short time history of the structures in the cross-sectional plane is given. Here, the structures are found by averaging the fields over a length of $3L_x$ in streamwise direction. By averaging over a region longer than the computational domain, the effect of the boundary conditions on the roll cells is taken into account. The velocity scale of the vortices in DNST was roughly half the value of DNSM.

In order to quantitatively compare the large-scale structures in the channel center, the two-point correlation coefficients of the streamwise velocity are plotted.

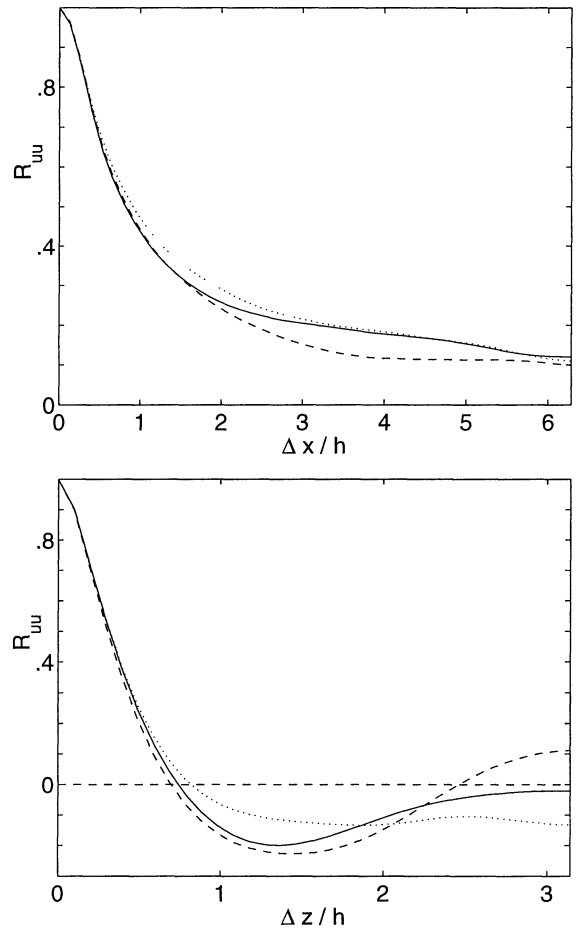


Figure 5: Two-point correlation coefficients in the streamwise direction (top) and spanwise direction (bottom). — DNSP (Kristoffersen et al., 1993), ... DNSM, — DNST.

ted in Figure 5. The evolution of the large-scale structures gave rise to a non-vanishing correlation coefficient $R_{uu}(\Delta x)$ at half the box length. DNSP and DNSM gave quite similar streamwise correlations, while DNST exhibited a lower correlation coefficient. This observation indicates that the elongated structures in DNST had slightly shorter streamwise extension. T-type boundary conditions suppress the tendency to form elongated structures in the streamwise direction.

The deviations between the spanwise correlations are more significant for the three DNSs (Figure 5). By defining the half streak width as the first minimum of $R_{uu}(\Delta z)$, the streakwidth in DNSM was $3.7h$ and in DNST $2.9h$. For DNSP the streak-spacing is $2.7h$ (Bech and Andersson, 1994). In addition to having wider streaks than DNSP, the correlation coefficient of DNST showed a clearer periodicity in the spanwise direction, meaning that the structures were more regularly spaced in the spanwise direction.

The mean velocity profiles of the two new simulations collapsed well with DNSP, as is seen in Figure 6. The difference in the large-scale structures had insignificant influence on this 1. order one-point statistics. The Reynolds number based on friction velocity, Re_τ , was for DNSM 82.5 and DNST 83.1, whereas for DNSP Re_τ was 83.5.

Root-mean-square values of the three fluctuating velocity components are given in Figure 7. The non-zero turbulent production rate in the channel center gives rise to high turbulent intensities here as compared to the pressure-driven channel flow. The deviations between DNSP, DNSM and DNST in the channel center can be due to the differences in the large-scale vortices. Some DNSs with strong secondary vortices have high level of $\overline{u^2}$ (Miyake et al., 1987; Lee and Kim, 1991; Bech and Andersson, 1994), while other simulations with less dominant secondary vortices (Bech et al., 1995; Komminaho et al., 1996) have lower values of $\overline{u^2}$ in the channel center. This can be explained by the secondary production of $\overline{u^2}$ caused by the vortices (Bech and Andersson, 1994). Therefore Figure 7 indicates that DNSM is more influenced by the vortices than DNSP, while in DNST the secondary vortical motion plays a less dominant role.

SUMMARY AND CONCLUDING REMARKS

Two new direct numerical simulations of turbulent plane Couette flow have been carried out. The customary periodic condition in streamwise direction was replaced by two new sets of repetitive boundary conditions. The first set consisted of taking the outflow as a mirror image of the inflow. In the second case the outflow field was set equal to the inflow field but translated a specified distance in spanwise direction.

The purpose of simulating the plane Couette flow using these boundary conditions was to study how they influenced the large-scale structures that are present in

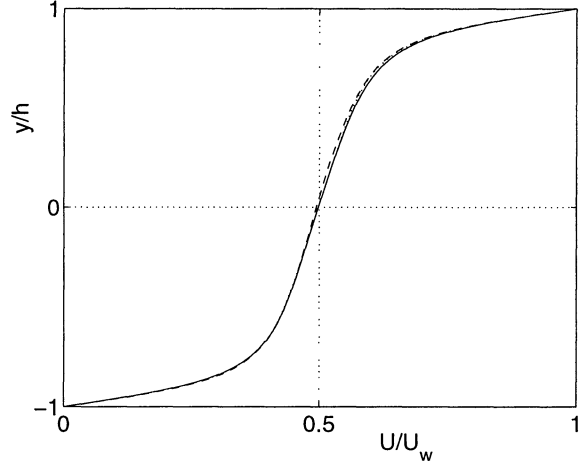


Figure 6: Mean velocity profiles.
— DNSP (Kristoffersen et al., 1993), ... DNSM,
-- DNST

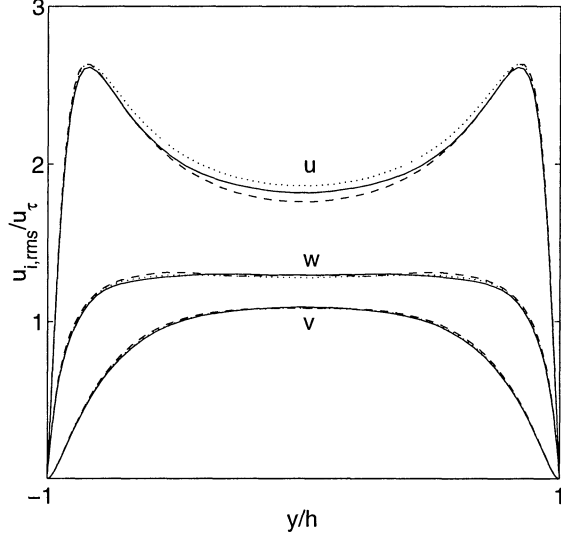


Figure 7: Turbulence intensities normalized with friction velocity. — DNSP (Kristoffersen et al., 1993), ... DNSM, -- DNST.

this flow. In the experiments by Bech et al. (1995) and Tillmark and Alfredsson (1998), elongated regions of high and low streamwise velocity have been observed periodically located in the spanwise direction. On the other hand, the presence of persistent counter-rotating pairs of roll cells have so far never been supported experimentally, even though the roll cells have showed up in different numerical simulations, as discussed in the introduction. The mirror-type boundary conditions allowed elongated structures to fill the whole streamwise length of the computational domain and this way giving them an infinite length. Pairs of roll cells did not show up in this simulation. The translation-type boundary conditions shortened the length of the streamwise streaks and strongly suppressed the tendency to form secondary vortices. These boundary conditions will efficiently prevent the roll cells to fill the whole length of the domain, as can be understood from Figure 1.

The computational domain used in the present simulations was too short to capture the extremely large streamwise scales observed in the experiments by Bech et al. (1995) and Tillmark and Alfredsson (1998). Like ordinary periodic boundary conditions, the two new sets of boundary conditions therefore intervene in the flow in a way that would not happen if the computational domain was much larger than the largest eddies in the flow. These large eddies make it extremely difficult to perform numerical simulations of this flow. No direct simulation known to the authors has captured the largest structures in the turbulent plane Couette flow. The computational domain in the simulations of Komminaho et al. (1996) had a length up to $28\pi h$. They nevertheless found a non-zero streamwise two-point correlation coefficient of the streamwise velocity at half channel length. Komminaho et al. (1996) pointed out that the use of periodic boundary conditions gives the correlation $R_{uu}(\Delta x)$ symmetry properties leading to the derivative of $R_{uu}(\Delta x)$ being zero at maximum separation. $R_{uu}(\Delta x)$ is therefore overpredicted at half the channel length. The translational boundary conditions do not have this symmetry property in streamwise direction. Therefore these boundary conditions can avoid the overprediction of correlations of velocities having large streamwise extension.

ACKNOWLEDGMENTS

This work has received support from The Research Council of Norway (Programme for Supercomputing) through a grant of computing time. ML was the recipient of a research fellowship offered by The Research Council of Norway under contract no. 115548/410. We appreciate the discussions with R. Kristoffersen during the course of this study.

REFERENCES

- Andersson, H. I., Lygren, M., and Kristoffersen, R., 1998, "Roll cells in turbulent plane Couette flow: Reality or artifact?" *16th International Conference on Numerical Methods in Fluid Dynamics*, Springer, pp. 117–122.
- Bech, K. H. and Andersson, H. I., 1994, "Very-large-scale structures in DNS," *Direct and Large-Eddy Simulation I*, Kluwer, pp. 13–24.
- Bech, K. H., Tillmark, N., Alfredsson, P. H., and Andersson, H. I., 1995, "An investigation of turbulent plane Couette flow at low Reynolds numbers," *J. Fluid Mech.*, Vol. 286, pp. 291–325.
- Bottin, S., Dauchot, O., Daviaud, F., and Manneville, P., 1998, "Experimental evidence of streamwise vortices as finite amplitude solutions in transitional plane Couette flow," *Phys. Fluids*, Vol. 10, pp. 2597–2607.
- Cherhabili, A. and Ehrenstein, U., 1997, "Finite-amplitude equilibrium states in plane Couette flow," *J. Fluid Mech.*, Vol. 342, pp. 159–177.
- Dauchot, O. and Daviaud, F., 1995, "Streamwise vortices in plane Couette flow," *Phys. Fluids*, Vol. 7, pp. 901–903.
- Gavrilakis, S., Tsai, H. M., Voke, P. R., and Leslie, D. C., 1986, "Large-eddy simulation of low Reynolds number channel flow by spectral and finite difference methods," *Notes on Numerical Fluid Mechanics*, Vieweg, Vol. 15, pp. 105–118.
- Kim, J., Moin, P., and Moser, R., 1987, "Turbulence statistics in fully developed channel flow at low Reynolds number," *J. Fluid Mech.*, Vol. 177, pp. 133–166.
- Komminaho, J., Lundbladh, A., and Johansson, A. V., 1996, "Very large structures in plane turbulent Couette flow," *J. Fluid Mech.*, Vol. 320, pp. 259–285.
- Kristoffersen, R., Bech, K. H., and Andersson, H. I., 1993, "Numerical study of turbulent plane Couette flow at low Reynolds number," *Appl. Sci. Res.*, Vol. 51, pp. 337–343.
- Lee, M. J. and Kim, J., 1991, "The structure of turbulence in a simulated plane Couette flow," *8th Symposium on Turbulent Shear Flows*, Munich, pp. 5.3.1–5.3.6.
- Miyake, Y., Kajishima, T., and Obana, S., 1987, "Direct numerical simulation of plane Couette flow at a transitional Reynolds number," *JSME Int. J.*, Vol. 30, pp. 57–65.
- Papavassiliou, D. V. and Hanratty, T. J., 1997, "Interpretation of large-scale structures observed in a turbulent plane Couette flow," *Int. J. Heat Fluid Flow*, Vol. 18, pp. 55–69.
- Tillmark, N. and Alfredsson, P. H., 1998, "Large scale structures in turbulent plane Couette flow," *Advances in Turbulence VII*, Kluwer, pp. 59–62.